adfm.200700888C

FULL PAPER

Biomaterials

M. K. Singh,* T. Shokuhfar, J. J. de Almeida Gracio, A. C. Mendes de Sousa, J. M. Da Fonte Fereira, H. Garmestani, S. Ahzi ■ 1–7

Hydroxyapatite Modified with Carbon Nanotube-Reinforced Poly(methyl methacrylate): A Novel Nanocomposite Material for Biomedical Applications

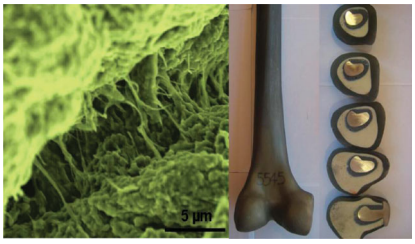

A novel nanocomposite designed for a new generation of biomedical bone cement and implant coatings is reported: the composite material consists of poly(-methyl methacrylate) (PMMA)-modified hydroxyapatite (HA) reinforced with multiwalled carbon nanotubes (see figure). The findings suggest that 0.1% of multi-walled carbon nanotubes in the PMMA/HA nanocomposite material gives the best mechanical properties

ADVANCED FUNCTIONAL MATERIALS

FULL PAPER

adfm.200700888

DOI: 10.1002/adfm.200700888

Hydroxyapatite Modified with Carbon Nanotube-Reinforced Poly(methyl methacrylate): A Novel Nanocomposite Material for Biomedical Applications**

By *Manoj Kumar Singh,** *Mrs. Tolou Shokuhfar, José Joaquim de Almeida Gracio, António Carlos Mendes de Sousa, José Maria Da Fonte Fereira, Hamid Garmestani,* and *Said Ahzi*

The paper reports on a freeze-granulation technique to prepare a novel nanocomposite of poly(methyl methacrylate) (PMMA)-modified hydroxyapatite (HA) with multiwalled carbon nanotubes (MWCNTs) as reinforcement for a new generation biomedical bone cement and implant coatings. By using this technique it is possible to increase material homogeneity and also enhance the dispersion of MWCNTs in the composite matrix. The phase composition and the surface morphology of the nanocomposite material were studied using X-ray diffraction, field-emission scanning electron microscopy, and micro-Raman spectroscopy. Additionally, nanomechanical properties of different concentrations of MWCNT-reinforced nanocomposite were performed by a nanoindentation technique, which indicates that a concentration of 0.1 wt % MWCNTs in the PMMA/HA nanocomposite material gives the best mechanical properties.

1. Introduction

Carbon nanotubes, because of their small dimensions and high aspect ratio, exhibit exceptional physical and chemical properties.[1–3] No other material can compete with their outstanding combination of mechanical, thermal, and electronic properties, which make them an outstanding reinforcement material for composites.[4–7] The ideal reinforcement material would impart mechanical integrity to the composite at high loadings, without diminishing its bioactivity.

Hydroxyapatite (HA) is the prime constituent of bone cements because of its ability to bond chemically with living bone tissues; this is due to its similar chemical composition and crystal structure to apatite in the human skeletal system. However, the intrinsic brittleness and poor strength of sintered HA restricts its clinical applications under load-bearing conditions.[8,9] Poly(methyl methacrylate) (PMMA) is another material commonly used as bone cement; however, its low mechanical strength makes the use of PMMA problematic. In the present work, a novel nanocomposite material was synthesized comprising multiwalled carbon nanotubes (MWCNTs), PMMA, and HA, which promises to be a superior material for biomedical applications. The selection of PMMA was made for two main reasons: i) PMMA is already used as bone cement and it is highly compatible with HA, and ii) MWCNTs are highly stable in their original form and PMMA can act as a functionalizing and linking material between them and HA.

There are two main goals when preparing the MWCNTs/PMMA/HA nanocomposite, namely: i) to obtain a homogenous dispersion of the MWCNTs, ensuring uniform properties throughout the composite, and ii) to enhance the interaction between the MWCNTs and mixing material to achieve an appropriate level of interfacial stress transfer. The dispersion of the MWCNTs is probably the most pressing issue. The MWCNTs should be uniformly dispersed to guarantee that they are individually coated with the PMMA-modified HA composite, which is imperative in order to have an efficient load transfer to the MWCNT network. This also results in a more uniform stress distribution and minimizes the presence of loci of high stress concentration. To this purpose, the percentage of MWCNTs in the nanocomposite material should be controlled—a large amount of MWCNTs cause them to bundle up in weakly interacting tubes as a result of the van der Waals attraction,[10] and, moreover, it will decrease the interfacial interaction between the mixing material and the MWCNTs.

Having these issues in mind, a freeze-granulation technique[11] is performed to prepare a novel nanocomposite of PMMA-modified hydroxyapatite with an appropriate percent-

[*] Dr. M. K. Singh, Mrs. T. Shokuhfar, Prof. J. J. de AlmeidaGracio, Prof. A. C. Mendes de Sousa
Centre for Mechanical Technology & Automation, University of Aveiro 3810-193 Aveiro (Portugal)
E-mail: mksingh@mec.ua.pt

Prof. J. M. da Fonte Fereira
CICECO, University of Aveiro 3810-193 Aveiro (Portugal)

Prof. H. Garmestani
Georgia Institute of Technology, Materials Science and Engineering 771 Ferst Drive, N.W. Love Building, Atlanta, GA 30332-0245 (USA)

Prof. S. Ahzi
University Louis Pasteur, IMFS-UMR7507 2 Rue Boussingault, 67000 Strasbourg (France)

[**] The financial support received from the Foundation of Science and Technology (FCT, Portugal) by two of the authors (M.K.S. and T.S.) is acknowledged. The present work was developed within the context of the research agreement signed between the University of Aveiro and Georgia Institute of Technology. Supporting Information is available online from Wiley InterScience or from the author.

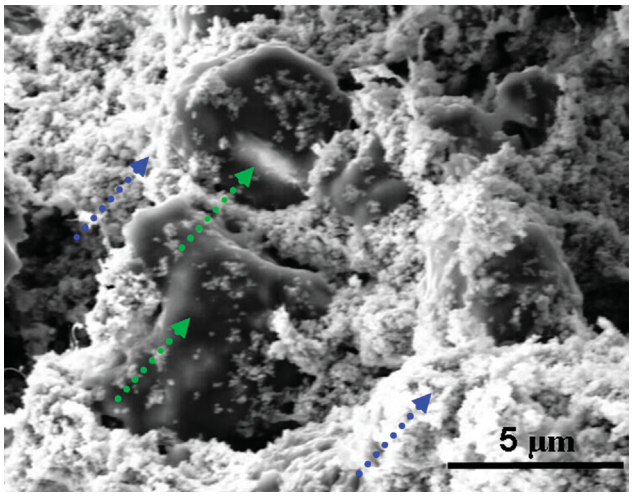

Figure 1. FE-SEM image showing the surface morphology of a 0.00% MWCNT–PMMA/HA nanocomposite, prepared by ball milling. The blue and green dotted arrows indicate HA and PMMA phases, respectively, in the PMMA/HA composite.

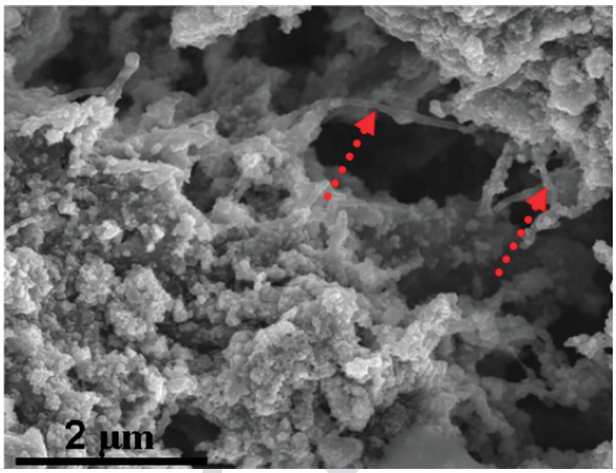

Figure 2. FE-SEM image showing the surface morphology of a 0.01% MWCNT–PMMA/HA nanocomposite prepared by freeze-granulation technique. From this image, it can be observed that some MWCNTs are sheathed with the PMMA/HA nanocomposite (indicated by a red dotted arrow).

age of MWCNTs. By using this technique it is possible to increase material homogeneity and also enhance the dispersion of MWCNTs in the composite matrix. The phase compositions and the surface morphology of the nanocomposite material were studied using X-ray diffraction (XRD), field-emission scanning electron microscopy (FE-SEM), and micro-Raman spectroscopy. Additionally, the determination of the elastic modulus and hardness of the nanocomposite was performed by a nanoindentation technique for a wide range of MWCNT concentrations. The tests indicate that 0.1 wt% concentration of MWCNTs in the PMMA-modified HA nanocomposite material yields the best mechanical properties. This novel nanocomposite material could be specifically used in bone cement that requires high strength and bone repair.

2. Results and Discussion

Figures 1–4 show the surface morphology of the MWCNT-reinforced samples for 0, 0.01, 0.1, and 1 wt% of MWCNTs, respectively. From the SEM observations for different concentrations of MWCNT-reinforced samples, it is clearly observed the concentration of 0.1 % of MWCNTs yields the best reinforcement for the PMMA/HA nanocomposite (Fig. 3a and b). For 0.1% MWCNT concentration, an intercalation of the PMMA/HA composite inside the MWCNT distribution does occur (Fig. 3a and b), leading to an increase in the MWCNTs' dispersion. Below this concentration, the mutual interaction between two adjacent MWCNTs is practically nonexistent, which tends to decrease the homogeneity of the nanotubes inside the PMMA/HA matrix. Figure 2 depicts the surface morphology of the 0.01% MWCNT–PMMA/HA nanocomposite. Higher nanotube concentrations, because less PMMA/HA is available to intercalate into the MWCNT distribution, may lead to weak bonding between the PMMA/HA and MWCNTs, making the composite weak in strength. The SEM image of 1% MWCNT–PMMA/HA composite shows agglomeration of MWCNTs into bundles. This indicates that the PMMA/HA did not intercalate into the bundles. Only the outside nanotubes of a bundle can be bonded to the composite (Fig. 4).

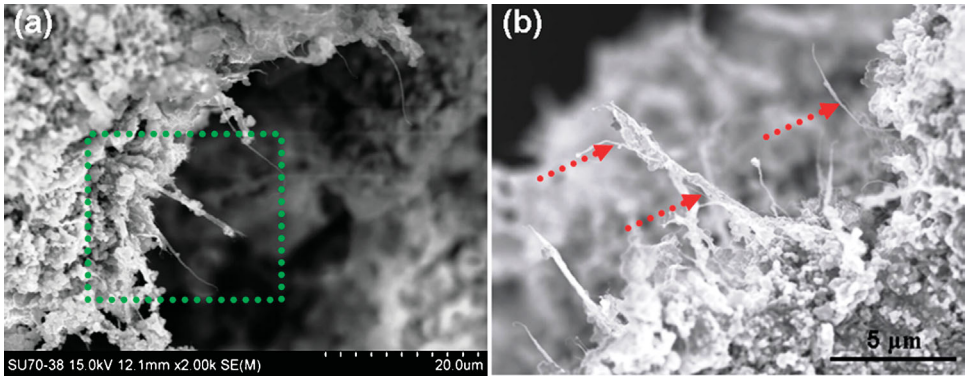

Figure 3. a) FE-SEM image showing the surface morphology of a 0.1% MWCNT–PMMA/HA nanocomposite. b) The highly magnified SEM image of the area denoted by a green dotted square in (a). The red dotted arrows point to isolated MWCNTs, which are completely covered by the PMMA/HA matrix.

Figure 5 illustrates the XRD patterns of PMMA, HA, and 0.1% MWCNT–PMMA/HA. It is clearly shown that the main constituent phases of the composite are crystalline HA[12,13] (Joint Committee on Powder Diffraction Standards, JCPDS card no.: 09-0432). No MWCNTs peaks were found in the XRD pattern of the 0.1% MWCNT–PMMA/HA compo-

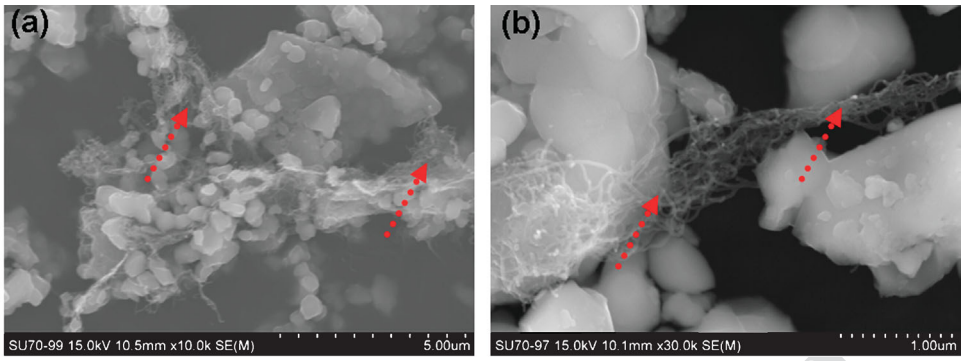

Figure 4. a,b) FE-SEM images taken at various locations of the 1% MWCNT–PMMA/HA composite sample, showing agglomeration of the MWCNT network (denoted by the red dotted arrows). This indicates that the PMMA/HA matrix did not intercalate into the nanotube network; therefore, only the outside nanotubes can bind to the composite.

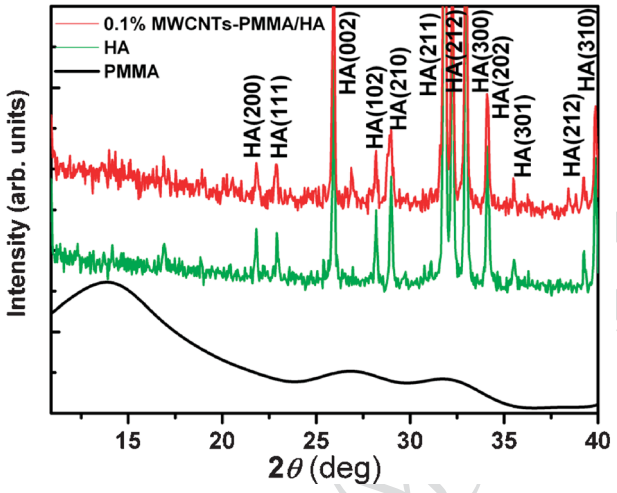

Figure 5. XRD results of PMMA, HA, and the 0.1% MWCNT– PMMA/HA composite. PMMA presents a broad amorphous peak at a 2θ value of 13°.

site, most likely because detection of small percentages of MWCNTs is not possible within the sensitivity limit of XRD. Miller indices of the diffraction peaks are given in parentheses in Figure 5. PMMA, which is an amorphous polymer (Meneghetti et al.[14]), shows a broad peak[15] at a 2θ value of 13°. The shape of the most intense broad peak reflects the ordered packing of the polymer chains.[15]

The visible Raman spectra collected from the 0.1% MWCNT-reinforced PMMA/HA sample, (an SEM image of which is shown in Fig. 6a) denoted by a blue line in Figure 6b, shows several distinct features. The feature near 1773 cm^{-1} is attributed to the C=O···O bonds and indicates that COO^- functional groups in functionalized MWCNTs interact with C=O of PMMA.[16–18] Several other peaks can also be observed at 602 (PO_4^{3-}), 962 (PO_4^{3-}), 1592 and 814 (tangential and symmetric CC_4 stretching modes, respectively), 1452 (CH bending), 1123 (C–O stretching), 1724 (–C=O stretching), and 2952 cm^{-1} (CH stretching), which are attributable to the HA, MWCNTs, and PMMA, as indicated in the figure.[19–23]

In the present work, the nanoindentation technique is employed to study the variation of mechanical properties of a MWCNT-reinforced PMMA/HA composite with different concentrations of MWCNTs. Figure 7 displays the typical load–displacement curves[24,25] at a peak indentation load of 10 mN on the MWCNT-reinforced PMMA/HA composite; it clearly demonstrates that no cracks were formed during indentation.[25,26] A considerable amount of creep strain at the peak load was found for all the samples. The holding segment at the peak load is necessary for the dissipation of creep displacement; most polymeric

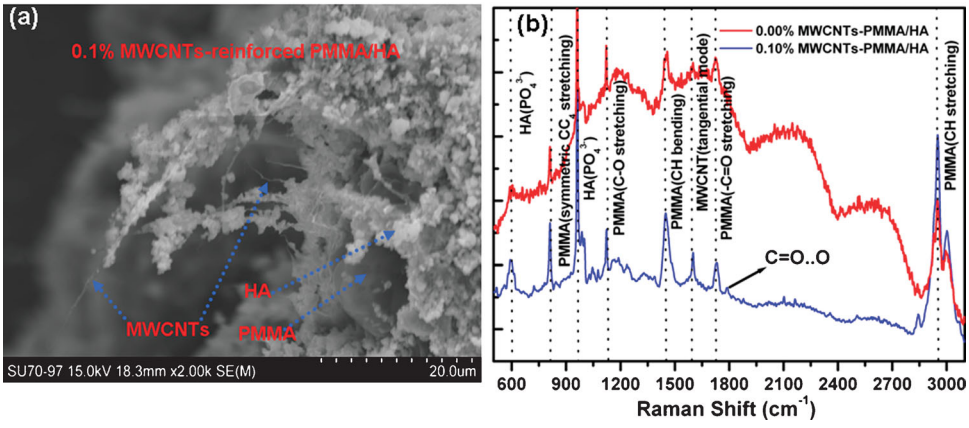

Figure 6. a) FE-SEM image of a 0.1% MWCNT-reinforced PMMA/HA sample prepared by the freeze- granulation technique. b) Raman spectra of PMMA/HA composites; the blue-line spectrum was collected from the sample shown in (a).

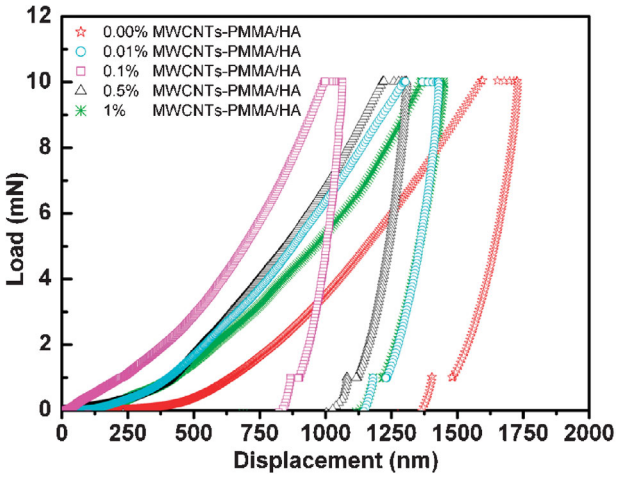

Figure 7. Typical load–displacement curves of indentations made at a peak indentation load of 10 mN on PMMA/HA nanocomposites with various amounts of MWCNT reinforcement.

biomaterials and tissues often exhibit this type of time-dependent or viscoelastic behavior.[27–30]

To study the effect of nanotube dispersion in the PMMA/HA composites, hardness and elastic modulus values are needed for both small and large indentation depths. Thirty two nanoindentation tests were carried out on each sample, and the experimental errors were ±0.60 GPa for the elastic modulus and ±0.05 GPa for the hardness. These values are presented in Figure 8 as a function of the indentation depth for PMMA/HA and its MWCNT-reinforced samples. The average hardness and elastic modulus for these composites are listed in Table 1. It can be observed that the hardness and elastic modulus of these composites increase with increasing MWCNT content up to 0.1%. Beyond this value, as can be noted from Figure 8a, an increase in MWCNT content yields a considerable decrease of hardness.

In a previous publication,[31] the authors demonstrated that there are several key requirements for an optimal fiber-reinforced, polymer-based composite system, namely: a) The fibers should be long enough so that the stress developed within them is significantly larger than the nominal stress on the composite; b) The cross-sectional area of the fiber should be as small as possible, as the strength of the fiber is inversely

Table 1. Average values of hardness (H) and elastic modulus (E) for different concentrations of MWCNTs in the PMMA/HA composites.

MWCNT Content [%]	0.00	0.01	0.1	0.5	1
H [GPa]	0.288	0.510	3.460	1.321	0.624
E [GPa]	5.949	14.022	69.528	28.08	10.56

proportional to the square root of its maximum flaw size; therefore, for smaller cross-sectional areas, the appearance of flaws is reduced; c) The spatial arrangement of the fibers in the matrix has to be of a significant order to ensure a unidirectional, maximal reinforcement. Also self-consistent calculations lead to the conclusion that an isotropic arrangement of the fibers will result in the dilution of the reinforcement effect within the polymer matrix. Previously, the law of volumetric mixtures was used to analyze the mechanical behavior of a continuous media of PMMA/HA with a blend of carbon nanotubes distributed in the matrix. According to the numerical calculations[32] carried out, the Young modulus of the composite increases with increasing MWCNT concentration up to a concentration of around 10%. The present experimental results show that above a concentration of 0.1% a noticeable decrease of the Young modulus is clearly identified (Fig. 8b). This discrepancy may be due to the fact that the modeling did not take into account two physical phenomena, which, in view of the experiments, are important, namely: 1) the interaction between nanotubes and 2) the character of the interface between the MWCNTs and the matrix. Increasing the MWCNTs concentration up to a certain level promotes a mutual interaction between a crossed pair or a coarse mesh of nanotubes (Fig. 9).

Consequently, the set of nanotubes can act as a deformation lock, either in extensional or shear mode, giving rise to improved mechanical properties. An identical behavior was noticed by analyzing the effect of the MWCNT concentration on a PMMA matrix.[33] It should be mentioned that the SEM images clearly show that after a concentration of 0.1% MWCNTs, a drop of homogeneity in the nanotubes–matrix contact occurs, giving rise to the formation of voids and internal cavities with the eventual reduction in the mechanical performance of the composite. In fact, most likely, these defects act as nucleation sites for internal crack tips and mutual link-up modes, with a fast degradation of the structure integrity and eventual breakdown. Fatigue tests were performed in artificial bones to confirm this analysis (Fig. 10). In the tests, after one million cycles, the nanocomposite of composition 0.1% MWCNT– PMMA/HA does not present any signal of crack propagation and delamination (Fig. 10a and b). But when we performed the same type of fatigue tests for PMMA-only nanocomposites, we can clearly observe delami-

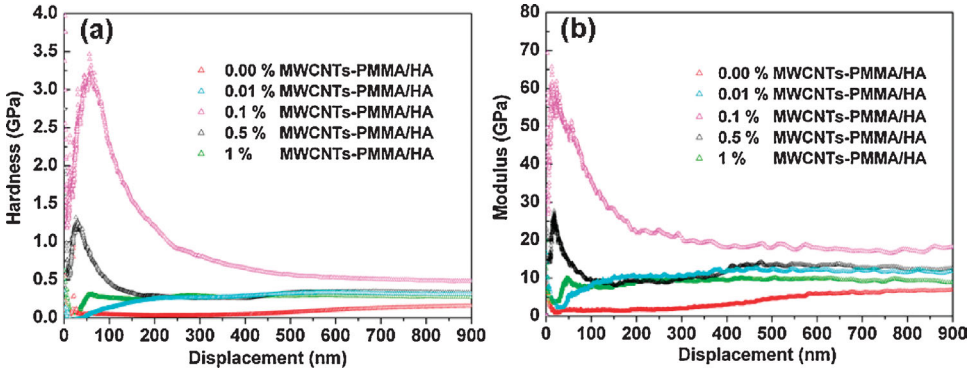

Figure 8. Hardness (a) and elastic modulus values (b) as a function of indentation depth.

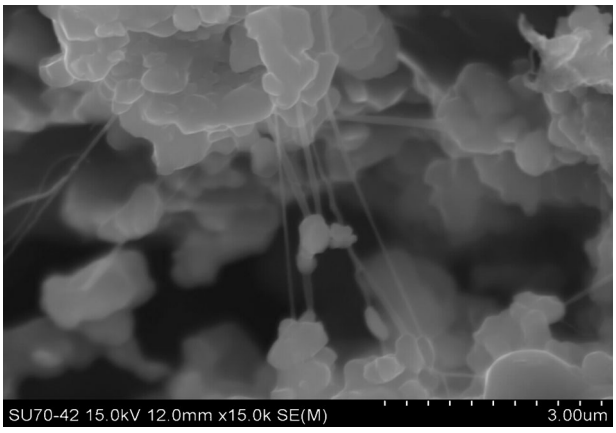

Figure 9. FE-SEM image showing interactions between crossed pairs of carbon nanotubes.

nation and cracks in Figure 10c and d, respectively.

3. Conclusion

Herein, we demonstrate a freeze-granulation technique to synthesis a novel nanocomposite of carbon-nanotube-reinforced PMMA/HA for next-generation biomedical applications. By using this method, it is possible to increase material homogeneity and also optimize the amount of MWCNTs in the PMMA/HA matrix. High-magnification SEM images (see Fig. 3) show that a concentration of 0.1% MWCNTs performs the best reinforcement for the PMMA/HA nanocomposites. The hardness and elastic modulus of MWCNT-reinforced PMMA/HA nanocomposites increase with increasing concentration of nanotubes up to around 0.1 wt%. Beyond this limit, further addition of MWCNTs to the PMMA/HA matrix yields a considerable decrease of these mechanical properties. This can be explained in terms of the nanotube–matrix contact homogeneity: a further increase of the amount of nanotubes may lead to the formation of voids and internal cavities, which can negatively impact the mechanical performance of the composite.

4. Experimental

Aqueous Dispersion of Functionalized Carbon Nanotubes: Commercially available (purity >95%, Nanocyl-3150) multiwalled carbon nanotubes with lengths of 1–5 μm and diameters of 5–10 nm were suspended in a 3:1 mixture of concentrated H_2SO_4 (18.4 M)/HNO_3(16 M) and sonicated in a water bath for 24 h. The resulting suspension was then diluted with water, and the MWCNTs were

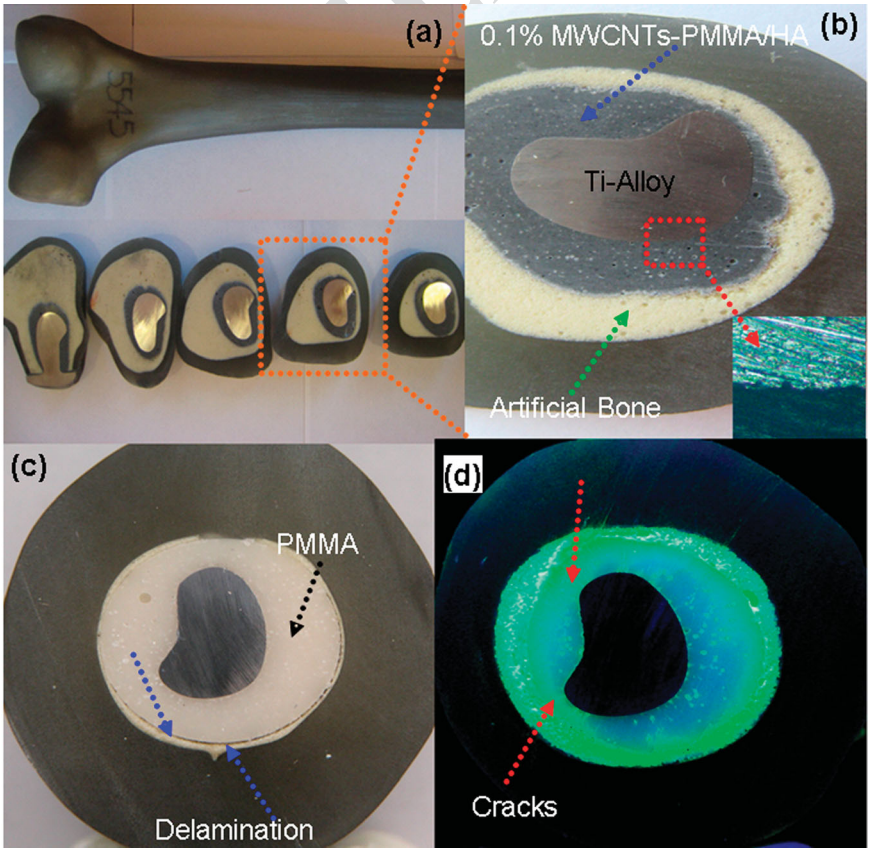

Figure 10. a,b) Optical microscopy observations of the 0.1% MWCNT–PMMA/HA nanocomposite at the interface with a titanium prosthesis after a fatigue test for one million cycles. c,d) Optical microscopy images showing delamination and cracks after the same type of fatigue test for a PMMA-only nanocomposite. ■[Q1]scale bars?■

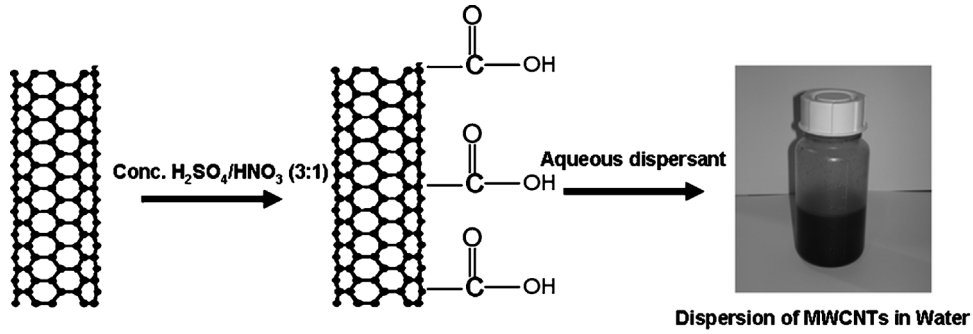

Figure 11. Schematic diagram showing the chemical functionalization of MWCNTs and their dispersion in water.

collected on a 100 nm pore membrane filter and washed with deionized water. The resultant functionalized MWCNTs (MWCNT–COOH) were investigated by Fourier transform IR (Nicolet AVATAR-360 FT-IR spectrophotometer) and visible micro-Raman (Jobyin Ivon T64000, $\lambda = 514.5$ nm) spectroscopies. IR spectra of COOH-functionalized MWCNTs showed the carbonyl stretching at 1729 cm^{-1} but in Raman spectra this signal was inactive. In Raman spectra a band centered at 1300 cm^{-1} was attributed to sp^3-hybridized carbon in the hexagonal framework of the nanotube walls. This disorder mode band was enhanced as functional groups were attached to the side walls of the nanotubes [34–38] (see Supporting Information S1 and S2). Acid–base titrations [39, 40] were performed to determine the concentration of COOH in acid-treated MWCNTs. The result indicated that around 3% carbon atoms were functionalized with COOH groups.

To obtain a homogeneous dispersion of MWCNT–COOH in water, an aqueous dispersant NanoSperse AQ (http://www.nano-lab.com/dispersant-suspensions.html) — a surfactant consisting mainly of poly(oxy-1,2-ethanediyl), tertramethyl-5-decyne-4,7-diol, and butoxy-ethanol — was used. The typical procedure involves mixing of 100 mg of MWCNT–COOH in 100 mL of distilled water with 4 mL of dispersant, and then keeping the mixture in a ultrasonication bath for one hour. The final product has a black color and no settling of MWCNTs is evident (Fig. 11).

Freeze-Granulation Technique to Produce the Nanocomposite of PMMA and HA with Dispersed MWCNTs: The well-dispersed MWCNT aqueous mixture was obtained for four different weight percentages of MWCNTs, namely, 0.01, 0.1, 0.5, and 1%. Each solution was mixed with a composite of commercially available PMMA (high-viscosity, bone-cement purity >99%, Johnson and Johnson Co.) and HA (particle size 2–3 μm with purity >98%, Agoramat-Advanced Materials) in 1:2 ratio by weight percentage. The homogenous mixture of HA powders and PMMA were prepared by ball milling. [41–43] There was no effect on HA powder size distribution during ball milling, thus, restricting agglomeration of HA powder during mixing of PMMA with HA. ■ok?■

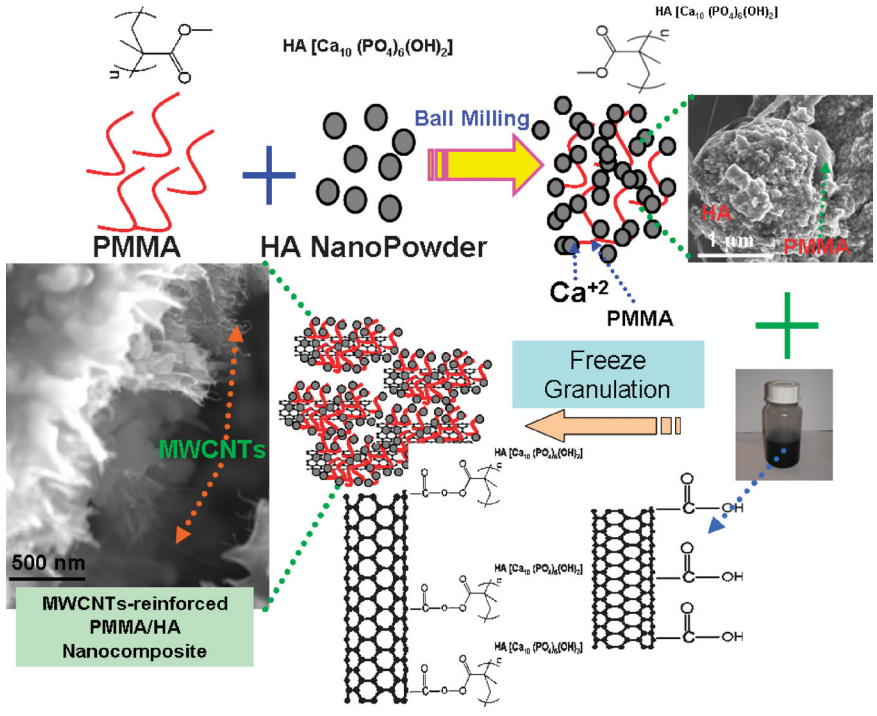

Figure 12. Schematic diagram for the formation of MWCNT-reinforced PMMA/HA nanocomposite by the freeze-granulation technique.

The freeze-granulation technique (Power Pro Freeze-granulator L5-2, Sweden) was performed with the objective of drying the nanocomposite of MWCNT-reinforced PMMA/HA powder to preserve the material homogeneity and enhance the dispersion of the nanoparticles in the composite matrix. Figure 12 shows the schematic diagram for the step-by-step freeze-granulation procedure, which yielded the synthesis of MWCNT-reinforced PMMA/HA nanocomposite. Granules with no cavities can be formed, and, without migration of small particles, a high degree of granule homogeneity can be achieved, while mild drying avoided oxidation of the powder. Also, lower granule density and the aid of evenly distributed low concentration MWCNTs will give softer granules with a wide granule size distribution. The freeze-dried nanoparticles were then collected and finally dried in vacuum for 3 days. In order to dry any remaining liquid the nanocomposite was kept for 24 h in the oven at 40 °C.

Surface Characterization: Field-emission scanning electron microscopy (Hitachi S-800, and SU-70, 30 keV) was performed to study the

dispersion and distribution of the MWCNTs in PMMA-modified HA matrix. The phase composition and purity of the samples were investigated by using a Philips Xpert-MPD X-ray powder diffractometer with Co Kα radiation at 45 kV and 40 mA. Room-temperature micro-Raman studies were also performed to study the integration of MWCNTs within the PMMA/HA nanocomposite material.

Mechanical Properties: Nanoindentation tests were performed using the MTS Nano Indenter XP with a Berkovich diamond tip. [24–26] The hardness and elastic modulus of the PMMA/HA nanocomposites with different MWCNT percentages were measured as a function of indentation depth using a continuous stiffness measurement (CSM) method. The typical nanoindentation test consists of seven subsequent steps: approaching the nanocomposite surface; determining the contact point; loading to peak load; holding the tip for 10 s at the peak load; unloading 90% of peak load; holding the tip for 100 s at 10% of the peak load for thermal-drift correction; and finally, unloading completely. The hardness and elastic modulus were obtained from the curves using the Oliver–Pharr method. [26].

Received: August 5, 2007
Revised: November 2, 2007
Published online:

[1] S. Iijima, *Nature* **1991**, *354*, 56.
[2] R. H. Baughman, A. A. Zakhidov, W. A. de Heer, *Science* **2002**, *787*, 297.
[3] H. Dai, *Surf. Sci.* **2002**, *500*, 218.
[4] G. Goller, H. Demirkiran, F. N. Oktar, E. Demirkesen, *Ceram. Int.* **2003**, *29*, 721.
[5] J. Cholpek, B. Czajkowska, B. Szaraniec, F. Beguin, *Carbon* **2006**, *44*, 1106.
[6] R. L. Price, M. C. Waid, K. M. Haberstroh, T. J. Webster, *Biomaterials* **2003**, *24*, 1877.
[7] A. Peigney, *Nat. Mater.* **2003**, *2*, 15.
[8] W. A. Curtin, B. W. Sheldon, *Mater. Today* **2004**, *7*, 44.
[9] A. A. White, S. M. Best, *Int. J. Appl. Ceram. Technol.* **2007**, *4*, 1.
[10] A. Kis, G. Csanyi, J.-P. Salvetat, T.-N. Lee, E. Couteau, A. J. Kulik, W. Benoit, J. Brugger, L. Forro, *Nat. Mater.* **2004**, *3*, 153.
[11] E. Liden, E. Carlstrom, L. Eklund, B. Nyberg, R. Carlsson, *J. Am. Ceram. Soc.* **1995**, *78*, 1761.
[12] S. Haque, I. Rehman, J. A. Darr, *Langmuir* **2007**, *23*, 6671.
[13] E. Bouyer, F. Gitzhofer, M. I. Boulos, *J. Mater. Sci.: Mater. Med.* **2000**, *11*, 523.
[14] P. Meneghetti, S. Quantubuddin, S. Webber, *Electrochim. Acta* **2004**, *49*, 4923.
[15] J. G. Ryu, S. W. Park, H. Kim, J. W. Lee, *Mater. Sci. Eng. C* **2004**, *24*, 285.
[16] C. Velasco-Santos, A. L. Martìnez-Hernández, F. T. Fisher, R. Ruoff, V. M. Castaño, *Chem. Mater.* **2003**, *15*, 4470.
[17] C. Velasco-Santos, A. L. Martìnez-Hernández, M. Lozada-Cassou, A. Alvarez-Castillo, V. M. Castaño, *Nanotechnology* **2002**, *13*, 495.
[18] J. M. Zhang, D. H. Zhang, D. Y. Shen, *Macromolecules* **2002**, *35*, 5140.
[19] M. Paillet, V. Jourdain, P. Poncharal, J. Sauvajol, J. C. Meyer, B. Chaudret, *J. Phys. Chem. B* **2004**, *108*, 17 112.
[20] F. F. M. de Mul, M. H. J. Hottenhuis, P. Bouter, J. Greve, J. Arends, J. J. Ten Bosch, *J. Dent. Res.* **1986**, *65*, 437.
[21] M. Suzuki, H. Kato, S. Wakumoto, *J. Dent. Res.* **1991**, *70*, 1092.
[22] S. Haque, I. Rehman, J. A. Darr, *Langmuir* **2007**, *23*, 6671.
[23] A. Matsushita, Y. Ren, K. Matsukawa, H. Inoue, Y. Minami, I. Noda, Y. Ozaki, *Vib. Spectrosc.* **2000**, *24*, 171.
[24] X. Li, B. Bhushan, *Mater. Charact.* **2002**, *48*, 11.
[25] B. Bhushan, X. Li, *Int. Mater. Rev.* **2003**, *48*, 125.
[26] W. C. Oliver, G. M. Pharr, *J. Mater. Res.* **1992**, *7*, 1564.
[27] S. Yang, Y. Zhang, *J. Appl. Phys.* **2004**, *95*, 3655.
[28] B. J. Briscoe, *Appl. Phys.* **1998**, *31*, 2395.
[29] B. Tang, A. H. W. Ngan, *J. Mater. Res.* **2003**, *18*, 1141.
[30] Y. T. Cheng, *J. Mater. Res.* **2005**, *20*, 3061.
[31] T. Shokuhfar, E. Titus, G. Cabral, A. C. M. Sousa, J. Gracio, W. Ahmed, T. I. T. Okpalugo, A. Makradi, S. Ahzi, *Int. J. Nanomanuf.* **2007** ■any update?■ in press.
[32] T. Shokuhfar, A. Makradi, E. Titus, G. Cabral, S. Ahzi, A. C. M. Sousa, S. Belouettar, J. Gracio, *J. Nanosci. Nanotechnol.* **2007** ■any update?■ in press.
[33] T. Akiskalos, M.Sc. Thesis, Massachusetts Institute of Technology, MA **2004**.
[34] Y. Ying, R. K. Saini, F. Liang, A. K. Sadana, W. E. Billups, *Org. Lett.* **2003**, *5*, 1471.
[35] C. A. Dyke, J. M. Tour, *J. Am. Chem. Soc.* **2003**, *125*, 1156.
[36] V. Georgakilas, D. Voulgaris, E. Vazquez, M. Prato, D. M. Guldi, A. Kukovecz, H. Kuzmany, *J. Am. Chem. Soc.* **2002**, *124*, *14*, 318.
[37] C. A. Duke, J. M. Tour, *Chem. Eur. J.* **2004**, *10*, 812.
[38] T. Wang, C. Tseng, *J. Appl. Polym. Sci.* **2007**, *105*, 1642.
[39] B. C. Satishkumar, A. Govindaraj, J. Mofokeng, G. N. Subbanna, C. N. R. Rao, *J. Phys. B* **1996**, *29*, 4925.
[40] S. C. Tsang, Y. K. Chen, P. J. F. Harris, M. L. H. Green, *Nature* **1994**, *372*, 159.
[41] Y. Chen, C. H. Gan, T. H. Zhang, G. Yu, P. Bai, A. Kaplan, *Appl. Phys. Lett.* **2005**, *86*, *251*, 905.
[42] A. M. Walker, Y. Tao, J. M. Torkelson, *Polymer* **2007**, *48*, 1066.
[43] N. Poudyal, B. Altuncevahir, V. Chakka, K. Chen, T. D. Black, J. Liu, Y. Ding, Z. L. Wang, *J. Phys. D: Appl. Phys.* **2004**, *37*, L45.

Q1: Please clarify throughout the article all editorial/technical requests marked by the black boxes.

*: Author please note that Figure 1-8, 10, 12 and TOC figure will be printed in color.

ADVANCED FUNCTIONAL MATERIALS

Postfach 10 11 61
69451 Weinheim
Germany

Courier services:
Boschstraße 12
69469 Weinheim
Germany

Tel.: (+49) 62 01 6 06 2 35 / 4 32
Fax: (+49) 62 01 6 06 5 00
E-mail: afm@wiley-vch.de

WILEY-VCH

Manuscript No. _____

Please correct your galley proofs and return them immediately.

The editors reserve the right to publish your article without your corrections if the proofs do not arrive in time.

Check the galley proofs very carefully, paying particular attention to the formulas, figures, numerical values, and tabulated data. A black box (■) or a question between black boxes signals unclear or missing information that specifically requires **your attention**. Note that the author is liable for damages arising from incorrect statements, including misprints.

Please limit corrections to errors already in the text; cost incurred for any further changes or additions will be charged to the author, unless such changes have been agreed upon by the editor.

Return the corrected proofs and the reprint order form by fax or mail (an address label is provided in the lower right-hand corner of this page for your convenience), or with the corrections integrated into the PDF file, to Wiley-VCH. Please do not send separate lists of corrections unless the position of each correction is also clearly marked on the galley proofs.

Fax: (+49) 6201 606 500

E-mail: afm@wiley-vch.de

Reprints may be ordered by filling out the accompanying form.

ADVANCED FUNCTIONAL MATERIALS

Boschstr. 12

69469 Weinheim
Germany

ADVANCED FUNCTIONAL MATERIALS

Postfach 10 11 61
69451 Weinheim
Germany
Courier services:
Boschstraße 12
69469 Weinheim
Germany
Tel.: (+49) 62 01 6 06 2 35 / 432
Fax: (+49) 62 01 6 06 5 00
E-mail: afm@wiley-vch.de

WILEY-VCH

Please complete this form and return it with your proofs.

Manuscript No. _____

Reprints/Issues

You have the opportunity to order reprints, issues or a PDF for an unlimited number of hardcopies at the quoted rates.

Reprints of *Advanced Functional Materials* articles are very popular. Whole issues, reprints, and high-quality PDFs are available at the rates given on a separate sheet. There is no surcharge for color reprints. After publication the prices of reprints are substantially higher. **For overseas orders please note that you will receive your issues/reprints by airmail. An appropriate surcharge will be levied to cover the higher postal rates. If you are interested in receiving the issues/reprints by surface mail please sign below.**

Please send me and bill me for

_____ reprints by ☐ surface mail
☐ FedEx
_____ entire issues by (FedEx No.:_____)

Mail reprints and/or issues to (no P.O. Boxes)

_____
_____
_____

Send bill to _____
_____
_____

VAT number _____

Tax-free charging can only be processed with the **VAT** number of the institute/company. To prevent delays with the processing, please provide us with the VAT number with this order.

Purchase Order No.: _____

Terms of payment:
☐ Please send an invoice ☐ Cheque is enclosed
Please charge my credit card
VISA ☐ MasterCard ☐ AMERICAN EXPRESS ☐ Expiry date ___/___
Card no. _____
Date, Signature _____

Cover Posters

Posters are available of all the published covers in two sizes (see attached price list).

☐ DIN A2 (42 x 60 cm/ 17 x 24in)

☐ DIN A1 (60 x 84 cm/ 24 x 33in)

PDF (unlimited number of hardcopies)

Please send me a bill for

☐ a PDF file (high resolution)

E-mail address _____

Please note: It is not permitted to present the PDF file on the web or on a company homepage.

★**Special Offer**★ If you order 200 or more reprints you will get a PDF file for half price.

_____ reprints and a PDF file

Mail bill to

_____
_____
_____

Subscriptions

As an author in *Advanced Functional Materials* you obviously appreciate the quality of the journal and value it as a medium for the distribution of your results. We thank you for this support. With the aim of ever increasing the dissemination of information we have maintained low (personal) subscription rates for *Advanced Functional Materials*. Please take advantage of these, ensuring yourself a regular supply of top information and helping us to keep subscription rates down and the accessibility of the journal up.

Please send me and bill me for

☐ the remaining issues of this volume
☐ the complete current volume
☐ the next year's volume
☐ a library subscription

Mail bill and journal to _____
_____
_____

Signature _____

Date _____

A4

WILEY-VCH

Price List for Reprints (2008)

The prices listed below are valid only for orders received in the course of 2008 and before the proofs pass for press. Minimum order is 50 copies. Delivery time will be approximately 3 weeks after the date of publication.

The production of reprints after a journal has been published is considerably more expensive, since it requires extra operations on the publisher's and printer's side. Therefore, authors are requested to order reprints early and in sufficient numbers.

If more than 500 copies are ordered, special prices are available upon request. **Single issues are available to authors at a reduced price.**

The prices include mailing and handling charges (with the exception of the additional costs incurred for airmail delivery and courier services). All Wiley-VCH prices are exclusive of VAT.

Reprints, posters, and issues for overseas orders are shipped by airmail (25.00 Euro surcharge). If you would like to receive them by surface mail please indicate this on the accompanying order form (postage for shipping posters within Europe: 15.00 Euro).

Reprints	Price for orders (in Euro)					
Size (pages)	50 copies	100 copies	150 copies	200 copies	300 copies	500 copies
1 – 4	266.–	312.–	361.–	408.–	502.–	689.–
5 – 8	381.–	450.–	516.–	583.–	718.–	987.–
9 – 12	494.–	580.–	668.–	754.–	930.–	1278.–
13 – 16	602.–	707.–	814.–	919.–	1132.–	1558.–
17 – 20	716.–	841.–	967.–	1095.–	1364.–	1851.–
for every additional 4 pages	114.–	133.–	152.–	172.–	211.–	289.–

Issues	1 copy: 17 Euro	**PDF (high resolution)**	300 Euro
Cover Posters	DIN A2 (42 x 60 cm/ 17 x 24in):	29 Euro	
	DIN A1 (60 x 84 cm/ 24 x 33in):	39 Euro	

★Special Offer★

If you order 200 or more reprints you will get a **PDF (high resolution)** for half price.

Annual subscription rates 2008

ADVANCED FUNCTIONAL MATERIALS

	Institutional (valid for print and electronic/ print or electronic delivery)	Personal rates (print only)
Europe	€ 3726.00 / 3387.00	€ 343.00
Switzerland	SFr 5883.00 / 5348.00	SFr 708.00
Outside Europe	US$ 4503.00 / 4093.00	US $ 468.00

Postage and handling charges included. All prices are subject to local VAT/ sales tax. Prices are subject to change.
Electronic products are delivered by Wiley Subscription Services Inc., 111 River Street, Hoboken, NJ 07030, USA,
VAT Registration No: EU826000141